Utrecht University

Natuur- en Sterrenkunde

Bachelor Thesis

Testing the pALPIDE v2 chip and researching module testing methods for the ALICE ITS upgrade

Author
Stan Oomen
Utrecht University
Student number - 4000315

Supervisors
Dr. Paul Kuijer
Nikhef
Dr. Panos Christakoglou
Nikhef
Dr. André Mischke
Utrecht University

June 15, 2016

Abstract

In the second Long Shutdown (LS2) of the LHC at CERN in 2018-2019, an upgrade of the one of the detectors, namely ALICE is planned to take place. A crucial part of the ALICE detector in identifying particles is Inner Tracking System (ITS). The main purpose of the ITS, which is the closest to the beam pipe, is to detect low momentum and short-lived particles. In the new ITS, a Monolithic Active Pixel Sensor architecture called the pALPIDE v2 is chosen to replace the current detector chips. A testing system for these chips including a MOSAIC board that converts the analogue to a digital signal that can be read out numerically by a computer has already been developed to test the chips. This setup also consists of a printing board that the chip is fixed on and a power supply. In the ITS, staves that consist of modules of 7 by 2 chips will be installed. Therefore it is necessary to be able to test multiple chips at once. Connecting multiple chips to each other and testing these modules as a whole is a delicate procedure since the silicon layers on the chip can easily be damaged. Two connection methods have been developed so far that are both undergoing a research en development phase. Firstly, the probing machine presses a single module down onto connector pins in order to make a connection and read out data for testing. Secondly, the FPC cutting machine cuts off a small strip at the end of a module to provide a connection using an external connector. In this process of cutting, the straightness of the cut is of utmost importance. In this bachelor thesis I have examined the possibilities for both the module testing methods as well as supplied a statistical analysis of a single chip in ROOT.

Contents

Chapter 1

Theoretical Overview

1.1 Standard Model

For decades, physicists have tried to unify all of the properties of the universe around us into one single equation or system. Until now, this has not been achieved due to the vast complexity of the matter and the interaction between the particles that make up the matter around us. One attempt at the unification of particles and their interactions into one theoretical framework is the Standard Model. The Standard model consists of 12 elementary particles and 4 forces at the moment. There is matter or spin 1/2 fermions that form the first three columns in the schematic overview below. The fourth column are the spin 0,1 or 2 bosons that mediate the forces between these particles. Particles are divided into two groups : quarks and leptons. They each consist of 6 particles which all have its antiparticle that have opposite quantum numbers. The difference between these quarks and leptons is that quarks interact via the strong nuclear force and the leptons do not. They are both divided into three generations, with each subsequent generation being a less stable particle. Generation 1 particles are the most stable thus making them the building blocks of everyday matter. Generation 2 and 3 particles are heavier and decay into lighter particles quickly.

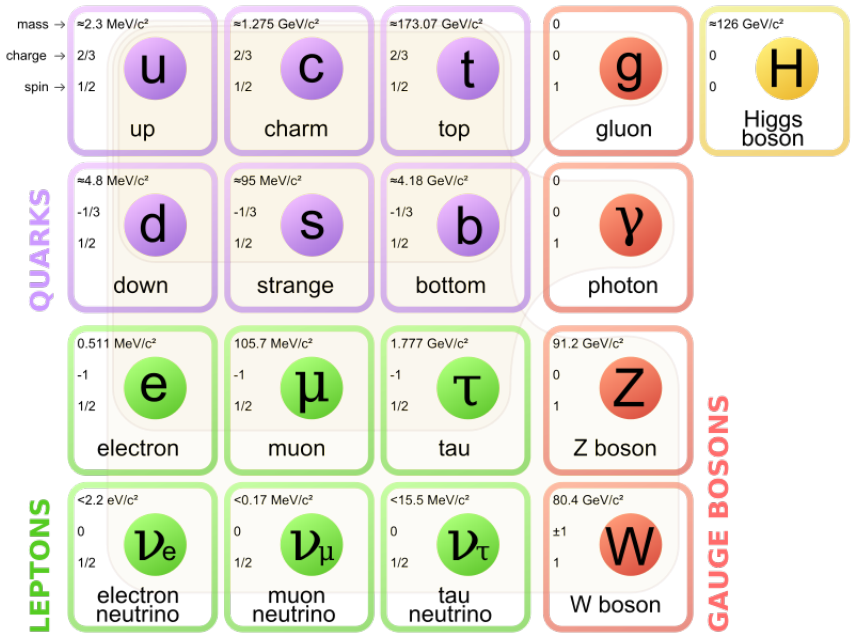

Figure 1.1 – The Standard Model of physics [1]

As mentioned earlier, there are 4 types of interactions between these particles. From strong to weak we have the strong interaction, the weak interaction, the electromagnetic force and gravitational force. All forces are mediated by their specific bosons. Bosons called gluons are the force carriers for the strong force that acts between quarks that make up protons and neutrons. This is by far the strongest force since it is in the order of 10^6 times stronger than the weak force yet it only acts on a small length scale in the order of the size of nucleons. [2] Quarks also have a special property called colour charge. Since their have a colour charge, they can interact via the strong interaction. This is where the realm of Quantum Chromo Dynamics comes in. But more on that in the next paragraph. For the weak interaction, Z^0 and $W^{\pm}$ bosons are the force mediators. All fermions can interact via the weak interaction. For electromagnetic interactions, virtual photons are the force carriers. The electromagnetic interaction only acts between particles that have an electric charge hence quarks, electron, muon and tau all interact electromagnetically. The last force carrier is one that is far less well know than the others, namely the Higgs-boson. It is known that all bosons are related to Gauge symmetries for the all interactions other than gravitational interaction. The Higgs bosons serves as a breaking of this symmetry. [3] This boson supposedly describes the interaction of the Higgs field with all the other particles. The Higgs field and the breaking of its symmetry is what generates mass for all the other particles. The associated Higgs boson was only recently found and is thought of to interact with the graviton, a spin 2 particle that has yet to be discovered and is supposedly responsible for mediating gravitational forces.

The Standard model is tested experimentally and seems self consistent in theory. [1] However, there are still physical phenomena that are not covered by the Standard Model such as Dark Matter and Energy which do not have their place in this model. Dark matter and Energy are believed to make up around 95% of matter and energy in the universe.[4] Another major deficit in the Standard Model is the question on where the mass of ordinary matter comes from. Quarks only make up around 1/100 of the mass of a proton or neutron, so it is largely unknown where the mass of these nucleons comes from. [2] This question is one of the main purposes of the ALICE detector, but more on that later. Overall, this attempt in unificating all particles and their interactions into one system is helpful, but far from complete.

1.2 Quantum Chromo Dynamics (QCD)

As mentioned before, the strong force is the force that keeps the neutrons and protons together inside of the nucleus although the protons are repulsive due to their positive electric charge. The strong force is the force that acts between quarks that have colour charge, hence the name Quantum Chromo Dynamics. QCD colour charge is similar to electrical charge in a sense that a particle with equal number of positive and negative charges is neutral in an electric way, and in the case of colour charge it is colour charge neutral. There are six colours, (anti-) red, (anti-)green and (anti-)blue. All mesons ($\bar{r}r, \bar{g}g, \bar{b}b$) and baryons ($rgb, \bar{r}\bar{g}\bar{b}$) are colour neutral, with the bar indicating an anti particle that has the same mass but opposite colour charge.[5] By exchanging gluons, quarks with different colour charges can interact. This is similar to electromagnetic interaction mediated by a photon at the speed of light, however gluons also carry charge themselves, so they interact with each other as well. There is one other significant difference between the strong force and other know forces. When the distance between two interacting quarks is increased, the force between them does not diminish like for instance an electromagnetic interaction decreases with distance. This creates the conditions that when quarks are pulled apart from each other, they instantly form a new quark - anti-quark pair due to a gluon field that is formed like a narrow tube (or string) of colour field between them.[6] This phenomenon that particles with colour charge such as quarks never appear in singularity is called confinement. At very short distances on the other hand, the strong coupling becomes small again, leading to asymtotic freedom of particles.

This quark model was very successful in organising all the states of hadrons but many physicists have long been sceptical of the existence of these quarks since they have never

been observed in a laboratory as free particles. Researching this phenomenon of free quarks, led to a discovery made in the early 1970's by Gross, Wilczek and Politzer when they discovered that QCD was asymtotically free. [6] Asymtotic freedom means that the strength of the strong coupling between particles decreases as the energy of a scattering experiment like ones that happen at the LHC is increased. The opposite also true for QCD, when the energy is decreased, the coupling becomes stronger. The first condition gives the opportunity for a Quark Gluon Plasma (QGP) to arise since confinement is no longer a necessity. The equations that govern QCD have not been solved analytically, hence a numerical approximation needs to be done in order to make calculations in QCD.

Numerical solutions of the equations of QCD can be approached in the form of Lattice QCD. In lattice QCD, a discretized lattice is introduced with a certain lattice spacing. On this lattice, observables can be calculated and with a infinitesimal lattice spacing and infinite lattice size, the continuum limit or analytical solution for QCD can be recovered again.[7] One of the major advantages of Lattice QCD is that numerical calculations can be done using Monte Carlo methods. These are methods used in computer calculations that use repeated random sampling in order to numerically calculate physical or mathematical models. Another advantage of Lattice QCD is that there is no limit to the scale of energy that is studied using QCD. These numerical calculations in the form of Lattice QCD are used to test whether or not QCD is a correct theory on strong interactions.

1.3 Quark Gluon Plasma (QGP)

The term Quark Gluon Plasma has been mentioned several times already in this thesis, however much is still unknown on whether or not this phase of hot QCD matter actually exists or not. This paragraph will cover the characteristics of a Quark Gluon Plasma and will address the question on whether or not it actually exists. At CERN in Geneva, heavy ion collisions generated by two beams of lead ions with centre of mass energies up to 5 TeV that are accelerated to nearly the speed of light by the LHC are examined by the different detector experiments. These heavy ions take on the form of a flat disk due to relativistic effects when being accelerated to nearly the speed of light. When the ion beams collide, not all the ions take part in a collision event because the collision is never completely head-on. The parameter that defines what percentage of the ion beams collide head on is called centrality, which has to be taken into account during data collection. The ions that do collide form an extremely hot fireball of deconfined quarks and gluons creating a phase of matter called a Quark Gluon Plasma. This phase of matter emerges only at temperatures in the order of trillions of Kelvins and extremely high densities as can be seen in the phase diagram below.

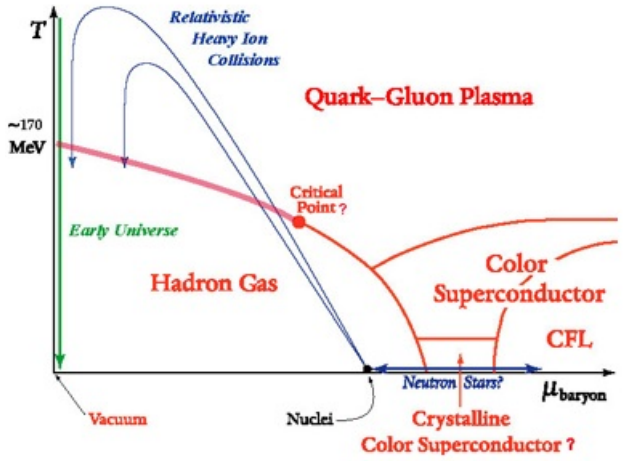

Figure 1.2 – The phase diagram which shows that a QGP is created only under extreme temperature and densities [8]

This hot and dense fireball instantly expands and cools and in this proces the individual quarks and gluons recombine into ordinary matter again that flies of in all directions creating showers of matter. Among the products of the recombination of the QGP, we can find particles such as pions and kaons, which are made of a quark and an antiquark. But also protons and neutrons, made of three quarks and even copious antiprotons and antineutrons, which may combine to form the nuclei of antiatoms as heavy as helium. [9]

Much can be learned from these particles and their distribution of energy since the characteristics of the particles that have been produced after the QGP has cooled down govern the properties of the QGP itself. The only properties that we can measure are the kinematics of the particles that are produced in these collisions and their interactions. According to QCD, high momentum particles produced in the initial stages of the nucleus-nucleus collisions will undergo multiple interactions inside the collision region before they hadronise into other particles. In these interactions with the QGP, their energy is reduced through collisions with the dense plasma and also through radiation. This effect is called jet quenching and is one of the main motivations of studying particles that are produced by a QGP since accurate reconstruction of jets will allow allow to determine the degree of quenching, thus providing more information on the interactions that happen inside the QGP. Examining these probes on their orientation, composition and jet quenching, it was discovered that unlike an ordinary plasma or gas, the QGP behaves more like a perfect Fermi fluid with a small viscosity. This enables the use of Quantum Chromo Dynamics to examine the QGP by looking at this strongly interacting matter and its characteristics such as temperature and viscosity.

Another way to study the properties of a QGP is to look at strangeness production. Strange quarks do not appear in ordinary matter that is constructed from up and down quarks that are present in the colliding ions. However, particles containing strange quarks are being detected by the inner detector elements in for instance the ALICE detector. Heavier charm and beauty quarks are also an interesting field of research. Hadrons containing these quarks are unstable and thus have a short life span. However, they can be detected by detector elements close to the beam pipe such as the Inner Tracking System in the ALICE detector. The next chapter will cover the different detector elements of the ALICE detector, especially focusing on the ITS and its purpose in pursuing the investigation of the QGP.

Now on to the question of whether or not the Quark Gluon Plamsa has been found or not. There is strong evidence that the effective degrees of freedom of the matter that is created in high energy collisions are not hadronic. In fact, fluid dynamics calculations have proven with the help of Lattice QCD that the number of degrees of freedom is much larger than one would expect from a hadron gas. This together with the argument that heavy flavour quarks have been detected suggests that a deconfined form of matter has existed in the hot fireball that is the QGP. Much research is still carried out at the moment on viscosity and sound speed measurements in the QGP in order to determine its characteristics more precisely. [10]

Chapter 2

Large Hardron Collider

2.1 Overview and Shutdown

The Large Hadron Collider is a particle accelerator that is located at CERN, close to Geneva in Switzerland. Its main architecture consist tunnel that is roughly 27 kilometres in circumference. In this tunnel, proton and lead ion beams are accelerated until they have an energy of 6.5 TeV and 2.51 TeV per nucleon respectively when they have a velocity that is close to the speed of light.[11] The general purpose of the LHC is to produce high energy proton collisions which can then be analysed by its different detector experiments along the circumference. This process takes place in multiple accelerators, starting with the LINAC2, which injects the ions into a booster ring where they gain momentum. From here the ion beam is injected into the Proton Synchrotron (PS) and successively the Super Proton Synchrotron (SPS). After this process, the ion beam is transferred to its destination, the LHC. At different locations in the LHC detectors such as the CMS, ATLAS, ALICE and LHCb are placed which all serve a different purpose in detecting particles after high energy collisions.

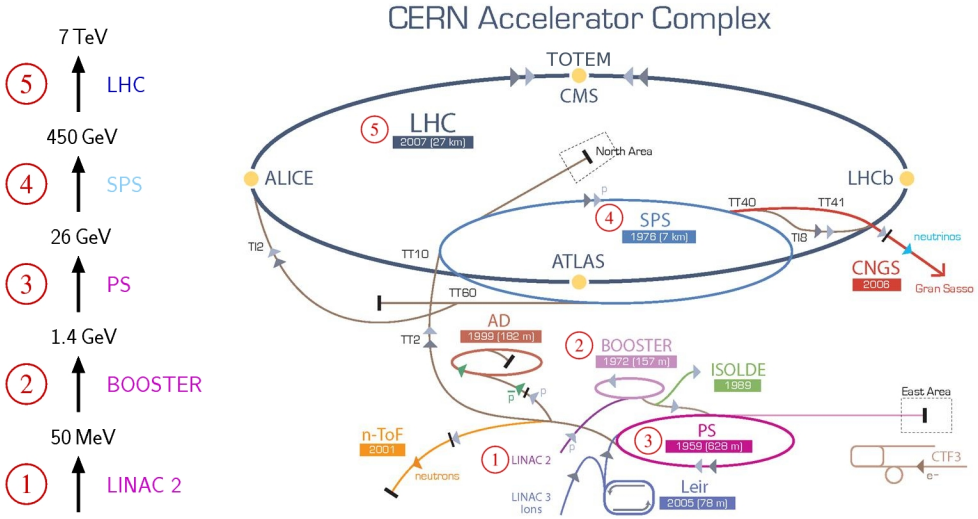

Figure 2.1 – Schematic overview of the LHC at CERN including ion beam energies at different stages of acceleration [12]

In 2018 and 2019, the second Long Shutdown (LS2) is planned for the LHC. This gives the opportunity to incorporate newly developed detector elements into the existing detectors, thus making it able to further examine the effects of the high energy collisions. My main concern in this process is the upgrade that takes place on the ITS or Inner Tracking System in the ALICE detector.

2.2 The ALICE detector - overview of different detector elements

As mentioned earlier, A Large Ion Collider Experiment or ALICE in short is one of the main detector experiments at CERN. Its general purpose is to study the strongly interacting matter and heavy-ion collisions, specifically a phase of matter called the Quark Gluons Plasma that can be formed under extreme pressure and temperature. ALICE is a collaboration from more that 130 institutes in 30 countries. The 10,000-tonne detector is 26 m long, 16 m high, and 16 m wide that is located in a vast cavern 56m below the ground receives high energy ion beams from the LHC and analyses the collisions with its multiple sub-detectors.[13]

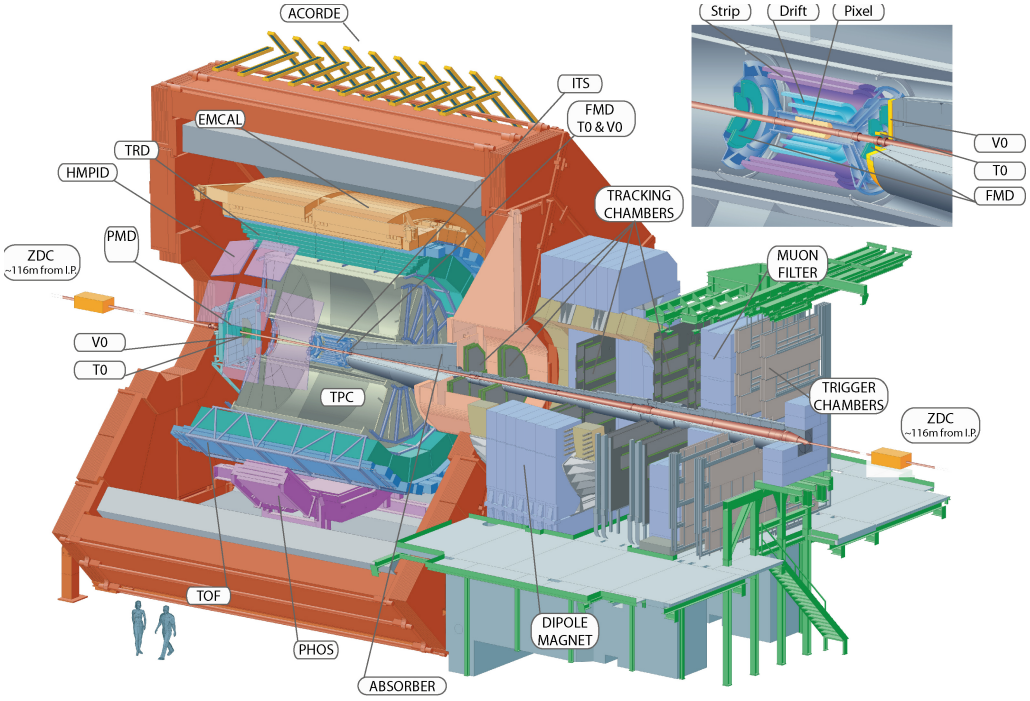

Figure 2.2 – Schematic overview of the ALICE detector at CERN including its sub-detectors around the central beam pipe [13]

In figure 2.2 a schematic overview of the whole ALICE detector is shown, including all of its sub-detectors. The largest structure in the detector is the L3 solenoid magnet which provides an almost completely homogeneous magnetic field parallel to the beam pipe, causing charged particles to travel in a curved path which is useful to calculate the momentum of particles. All different detector elements have their own specific function and optimised design for that purpose. From the beam pipe outwards we have the Inner Tracking System (ITS) which precisely tracks the location of passing particles, the Time Projection Chamber (TPC) which also tracks particles using a gas filled volume and Time Of Flight (TOF) which calculates the velocity of incoming particles. In the outer shells of the ALICE detector we find calorimeters such as PHOS and EMCal which determine the energy of particles that reach the outer layers of the ALICE detector.

All these detector elements have to work together since the data from one of the inner detectors can be useful when compared to the data that is gathered by the outer detector elements. The main concern of this thesis is the inner most detector element, the Inner Tracking System. The following sections will cover the current ITS and its planned upgrades.

The ALICE detectors main concern is detecting the remains of the extremely hot QCD matter that created heavy ion collisions. When a Quark Gluon Plasma is created,

it quickly want to reach equilibrium by expanding and cooling down. In this process, heavy particles are created as mentioned before. These heavy particles such as D^0 mesons have a short decay time. Hence, the only way to physically analyse these particles is by tracking the paths of the decay products. This is done by the inner detector elements of the ALICE detector.

2.3 Current ITS - main purpose and limitations

The ITS is the detector element that is the first thing particles encounter after collisions since the ITS is closest to the beam pipe. The main function of the ITS is high precision tracking of particles and their primary and secondary vertices. These reconstructions of particle tracks is used to study heavy flavour particles such as the D^0 meson that decay quickly since only their decay products can be measured directly. Also, the ITS has a special feature in detecting low momentum particles and how they are scattered by determining the impact parameter as precisely as possible.

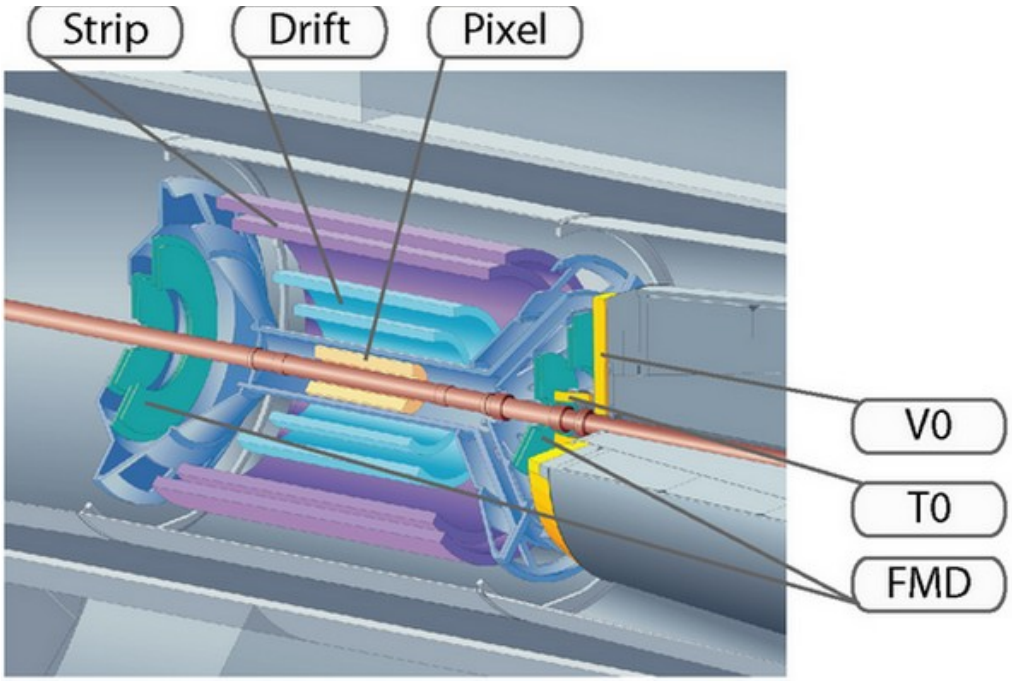

Figure 2.3 – Schematic overview of the Inner Tracking System inside the ALICE detector [14]

The above schematic shows that there are 6 concentrical and cylindrical detector layers that make up the ITS. Starting with the silicon layer closest to the collision area there are 2 layers of SPD (Silicon Pixel Detector), 2 layers of SDD (Silicon Drift Detector) and finally 2 layers of SSD (Silicon Strip Detector). Overall, the inner and outermost layers are placed at 3.9 cm and 43.0 cm respectively and has a pseudorapidity coverage of $|\eta| < 0.9$ [15].

The inner two layers of SPDs are essential for determining the exact location of the collision otherwise called the primary vertex. These type of silicon pixel detectors were chosen for the layer closest to the beam pipe since they have a high pixel count. This makes them ideal for particle detection close to the beam pipe since the particle density is highest there. Currently the whole ITS is designed for up to 100 particles per cm^2 for Pb-Pb collisions at $\sqrt{^S NN} = 5.5$ TeV. In order to achieve the desired precision for these high particle densities, the SPD are essential. Also, the distance of the SPD's to the beam pipe was lowered to the minimum allowed by the beam pipe in order to provide high precision in the determination of the primary vertex and precise tracking in combination

with the TPC. The four outer layers, the SDD and SSD, have to have different specifications because the particle density has fallen to up to 1 particle per cm^2 in the outer layers. The outer layers are double sided and have analogue read-out and can be used for particle identification (PID) via dE/dx measurements in the non-relativistic $1/\beta^2$ region.

A crucial limitation of the present ITS detector is given by its inability to provide sufficient statistical significance to study the production of charm mesons at low momenta. This especially accounts for charm baryons that has a decay length of only $60\mu m$. This is lower than the current impact parameter resolution of the current ITS in the case of transverse momentum range for its daughter particles. The lack of resolution makes it that these particles like beauty mesons, beauty baryons and heavy quark hadrons that could reveal a lot about the characteristics of the QGP can not be detected by the current ITS.

Another limitation that the current ITS has is its limited read out time which is the rate at which a pixel can detect a particle and reset itself to get ready to detect another hit. The sheer amount of particles produced in Pb-Pb collisions can reach at frequency of 8 kHz, which is much higher that the read out rate of the chips in the ITS which is around 1 kHz. So it can only use a small fraction of data from the collisions that happen in the beam pipe.

Overall, it is clear that the current ITS is not adequately equipped fully analyse all the collisions that take place within the LHC due to its limitations is resolution and read out frequency. These factors are planned to be improved upon, which will be the subject of the next paragraph.

2.4 ITS upgrade

We have seen in the previous paragraph that there are still some limitation on the capabilities of the ITS in ALICE. The LS2 or Long Shutdown 2 in 2018-19 will give the opportunity for major upgrades to take place. With these upgrades, more precise measurements can be done which enhances the possibilities of researching particle physics and in special the Quark Gluon Plasma. In the schematic below, the upgraded ITS is displayed including more detailed schematics of the inner- and outer barrels.

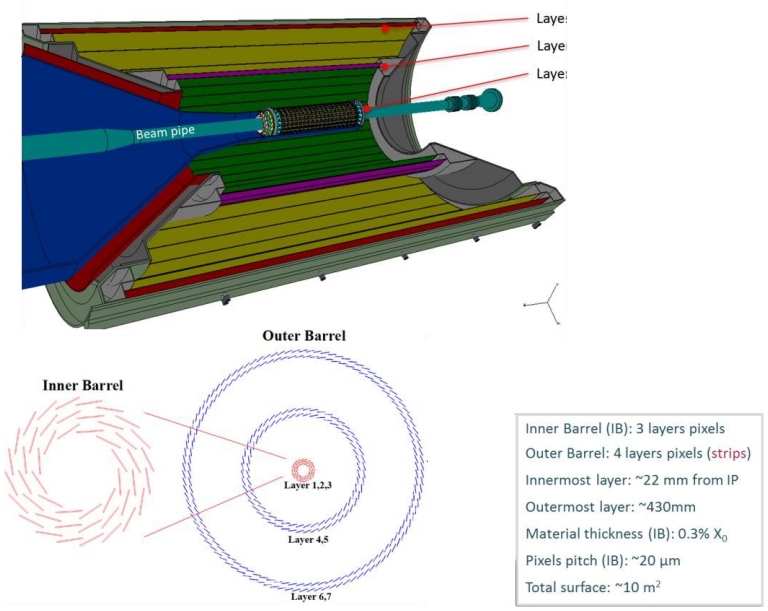

Figure 2.4 – Overview of the upgraded ITS detector element in ALICE [16]

One upgrade that can be seen immediately is the addition of a seventh pixel chip

layer. An extra layer in the inner barrel (IB) will provide a better resolution in measuring transverse momenta and impact parameters. All the silicon detector layers will be replaced by ALPIDE silicon pixel detectors instead of the original SPD, SDD and SSD. The pixel size will therefore be decreased to 30 x 30 μm^2 compared to 50 x 435 μm^2 in the current pixel detector elements. The active pixel surface will be approximately 10m^2 with a total of 12.5 billion pixels.[15]

The inner design of the upgraded ITS will be somewhat different from its predecessor. All the ALPIDE chips are mounted on a lightweight Space frame which is the support structure for a single stave based on carbon fibre. Around the pipes we can find the Cold plate, a carbon structure that lies around the pipes used for cooling. Since the electronics in the pixel chips generate heat, this heat has to be dissipated in order to assure that the pixel chips are working under stable temperatures. The Hybrid integrated Circuit consists of a flexible printed circuit (FPC) on which 2 times 7 Pixel chips are assembled. The FPC is the way for the pixel chip to transmit their data to the the data servers of the ALICE experiment and is designed in order to transmit data as fast as possible while maintaining a low material budget. The assembly of the modules from the 14 single pixel chips is a delicate process. Since all the modules have a silicon top layer which can be damaged easily, these modules have to be handled with caution. Also, testing these modules prior to installing them in the actual ITS is a matter of its own. Chapter 4 will cover how these modules are prepared for testing and what challenges lie ahead to producing mass scale testing apparatuses that are easy to handle and quick to test a whole range of modules. In the figure below, a schematic overview of the new architecture of what the upgraded ITS will look like.

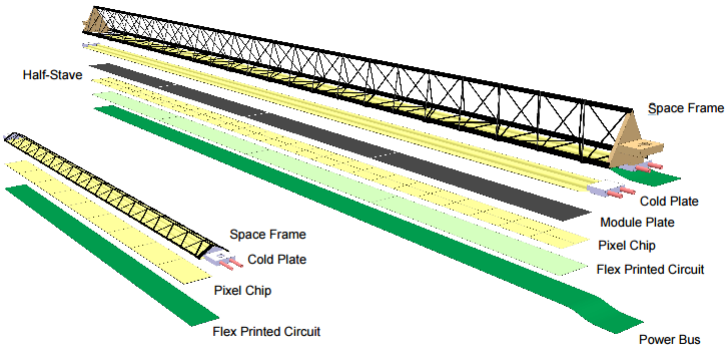

Figure 2.5 – Structure of staves that make up the layers of the ITS. Left for the Inner Barrel, right for the Outer Barrel [15]

The primary focus of the upgrade of the ITS lies on better detection of heavy-flavour hadrons that are produced when a QGP is created. One major upgrade to support this wish is the reduction of the distance of the first detector element to the beam pipe. This upgrade will provide a better impact parameter resolution determination for particles which have short decay times. Current studies indicate that it is possible to get to a distance of 17.2 mm to the beam pipe, compared to the current 29 mm.

A crucial in the upgrade of the ITS in order to optimise it for low transverse momenta is a low mass of the three innermost layer, which will have a material thickness of 0.3% X_0 per layer. The outer and middle layers 0.9% X_0 compared to 1.14% X_0 per layer in the current SPD.[15] The reason the reduction of the material budget is important is that every time a particle goes through a detection layer it loses some of its energy and momentum. So in order to obtain precise measurement, the interaction of particles with the SPD layer has to be minimised. This is particularly important when measuring low momentum particles in a precise way since the interaction these particles have is mostly due to Coulomb scattering. The use of Monolithic Active Pixel Sensors (MAPS) will allow the silicon material budget per layer to be reduced in comparison to the present ITS with a thickness per chip of 50 μm instead of 350 μm per chip.[15]

Overall, the SPD's have to perform under demanding conditions so the requirements for the pixel chips are very high. As we have seen in this chapter, the pixel chips have to have a high resolution, low power consumption and low material budget. SPD's perform well in these areas. However, there is still one major disadvantage to using silicon pixel detectors namely the read out speed that it has. The read-out time is the amount of time it takes for the detection system to transmit its data to the read out system. In between two successive interactions with particles, the pixel has to reset and transmit its data through the read out system. Minimisation of this read out time is therefore essential in high frequencies of interacting particles but also in comparing whether or not two particles have hit a silicon chip simultaneously at different positions. The present ITS features a maximum read-out rate of 1 kHz. The next ITS is designed to interpret data from each individual interaction up to 100 kHz for Pb-Pb collisions and 400 kHz for p-p collisions. A rate which is twice as high as the requirements from ALICE group, just to ensure proper data read out at high frequencies.

2.5 ALPIDE Chip

Several different types of chips have been tested in order to find out which one will have the best specifications for operating in the ITS. The only relevant information that the pixels in the ITS have to supply is whether or not a particle has interacted with the pixel. In order to make sure that there are no false detections, the information that the pixel gathers is compared to a threshold. Then all the data has to be read out, and this is where proposed chip architectures like MINSTRAL, CHERWELL, ASTRAL and ALPIDE differ from each other. The most used way of reading out a pixel chip is the rolling shutter method and use a comparator at the end of each column. Yet, the ALPIDE chip uses a different scheme for reading out information. It contains a newly developed low-power circuit which is installed in the pixel itself. This drives a system that stores the data of all the addresses of the pixels. This is in turn read out by a data compression circuit at the end of each column. The digitisation of the signal within the pixel eliminates the need for an analogue column driver, reduces the power consumption significantly and allows for fast read-out. [15] In contrast to the other read out techniques, whenever a hit takes place, it is stored in the pixel chips memory, therefore eliminating the need for analogue read out which enables te read out time to be shortened and power consumption to be lowered. This chip architecture enables the integration time to be significantly lower compared to the MINSTRAL with 4 μs compared to 30μs (MISTRAL, CHERWELL) and 20 μs (ASTRAL). Also, the power consumption is much lower with 50 mW cm^2 compared to 200 mW cm^2 of the MINSTRAL, 85 mW cm^2 for the ASTRAL and 90 mW cm^2 for the CHERWELL structure. [15]

The final version of the ALPIDE chip is still undergoing a phase of research and development, yet several prototypes have already been produced and are being tested at the moment. One of those prototypes is installed at Nikhef as a part of an experimental setup. Here we are testing this pALPIDE v2 chip to see if it meets the standards that are set by the ALICE group. Since the ALPIDE chip at Nikhef is still a prototype, it is not yet optimised and therefore the testing of this single chip only gives an indication of the capabilities of the final version of the ALPIDE chip that will eventually be installed in the ITS. Of course, it will not be the single ALPIDE chips that will be installed, but whole modules that are assembled into staves. The next chapters will cover the testing procedure of a single chip including noise and threshold measurements (Chapter 3) and the challenges that arise when whole staves have to be tested for the same properties. Two different connection methods have been under development for the last months, namely the Probing machine and the Cutting machine. They both have different advantages and disadvantages when it comes to testing whole modules. This will be covered in Chapter 4.

Chapter 3

Chip testing

The ALPIDE pixel chip has been chosen as the chip that will eventually be installed in the ITS. However, before the final version of the pixel chip is ready to perform adequately, several prototypes have to be tested at the different institutes that contribute to the development of the ALPIDE chip.

3.1 Experimental Setup at Nikhef

This experimental setup for testing a single has been set up during a Bachelor projects before mine by Pim Verschuuren[17] and Lukas Arts[18]. They provided a power supply grid to the pALPIDE v2 chip that is placed on an FPC. This power supply was especially designed in order not to not damage the pixel chip by applying an amperage that is too high. A green LED was installed which acts as a 1.8 Volt limit. [17] More safety features such as a an electrical resistance and coils are installed in order to lower the interference of the power signal. Using a data cable that can regulate all three Low Voltage Differential Signals called CLK, CNTR and DATA, the data is supplied to a FMC port on the MOSAIC board. [17] The MOSAIC board is especially designed to test pixel chips that are used in particle detections. The signal from the MOSAIC board is in turn used to further transmit the data through an ethernet cable to the computer at Nikhef. Here previously written software can be run to receive and store data from measurements. Also, in the Graphical User Interface of this program, several test can be performed such as a Threshold and Register test with parameters that can be set by the user. The threshold test measures the amount of voltage has to be applied to a pixel in order for it to register a hit. The register test assigns different values for pixels in one of the 8 sub matrices and these binary values are subsequently read out again to see if a different result is generated as output by the memory registers. This test is only performed to be sure that all the sub matrices of the pixel work correctly. The firmware of the MOSAIC board has been updated during the course of my bachelor research and has been successively installed.

At the heart of the experimental setup at Nikhef is of course the chip itself, the ALPIDE chip. It measures about 15 by 30 mm and contains a pixel array of 512 rows by 1024 columns of pixels that have dimensions 22μm by 22μm. This is one of the first prototype matrices of ALPIDE. As mentioned before, each pixel has a built in digital function that compares the incoming hit with a threshold in order to determine whether or not a hit needs to be registered. When a pixel is hit, this is stored in the internal memory of the pixel as a binary 1. Of course, when no hit is registered that goes above the threshold, the one bit memory stays at 0. An internal clock cylce which runs at 10 MHz reads out and resets all columns and rows in order to make sure that all relevant pixels are read out before it resets. [19] The pixel state register is read out by the Address Encoder and Reset Decoder(AERD) circuit that is arranged per column. This stores only the address of the hit pixel and sends it to the periphery of the chip, leaving out the pixels that have a binary value of 0. Therefore, the pixel speed read out is proportional to the number of hits the pixel chip registers.

Furthermore, the chip is divided in 4 sub matrices that are each 512 rows and 256 columns. Each of these different sectors has a different sensor layout and have different reset mechanisms. We will see in our measurements that these four matrices all perform somewhat differently when doing measurements.

3.2 ROOT Analysis

The analysis of the data start by gathering raw data from the pALPIDE v2 chip using the program that was previously written by Lukas[18] This exports a long list of data lines that is structured with each row consisting of the location of the pixel, the DAC steps and the threshold. These DAC steps are internally generated increasing voltages of the injection signal with which we can calculate the threshold of the different pixels. Using the scientific data analysing software ROOT 5.34, the large data file can be visualised using multiple lines of code in C++. Hence I wrote a ROOT script which visualises data I have gathered myself from the experimental setup. To provide the best statistical analysis possible, I have let the program run its data gathering procedure for quite a while, gathering more than 200.000 lines of data in the process. The data was gathered with a closed box around the pixel chip in order to prevent any outside factors from influencing the measurements.

3.3 Threshold Measurements

As mentioned before, the threshold of a certain pixel is the amount of charge that has to be applied to the pixel in order for it to register a hit. Ideally, this will be a Heavyside Step function since there is a certain value of charge at which a pixel should register a hit. Unfortunately, this can not be achieved exactly because of thermal and electrical fluctuations in the pixel which cause noise. In the experiment, it is not particles that are used to simulate the conditions in the ITS. In fact, the pixel chip is covered with a box that eliminates the influence of incoming light or particles from the room. The threshold scan is simulated by an internal Digital to Analogue Converter (DAC). This DAC can be set to increase the voltage on a pixel with a certain predetermined amount of steps in order to research the threshold. The figure below shows a threshold analysation of the first pixel matrix.

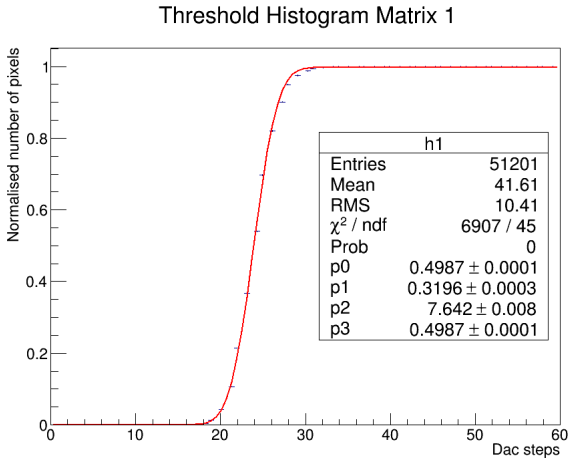

Figure 3.1 – The threshold scan visualised for the first pixel matrix

The data is fitted to an error function with variables that have been found by trial and error. As can be seen, the threshold is not a perfect Heavy Side step function as expected. However, threshold is around DAC step 26 from the 60 steps. Now we can analyse the thresholds of all pixels in the four different matrices of the pixel chip. Then they are compared to each other in a histogram.

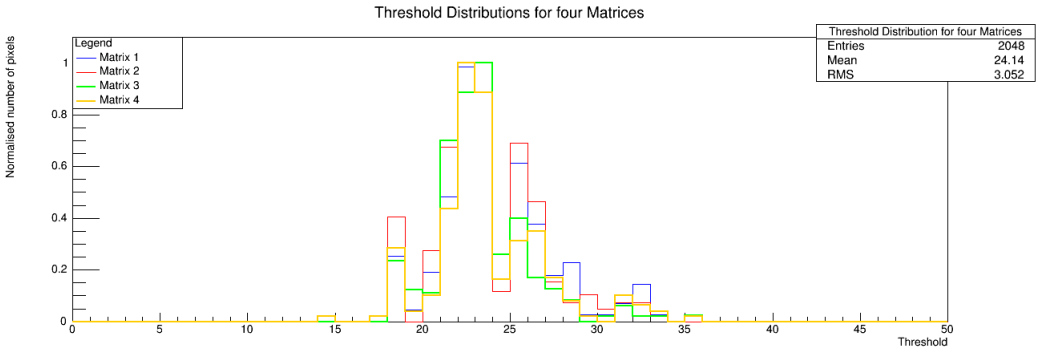

Figure 3.2 – The threshold distribution for different pixel matrices

In this figure, the amount of pixel has been normalised to in order to compare the different pixel matrices. In total, 20475 pixels were tested. From this we can conclude that the threshold distributions are similar in all the different pixel matrices. Comparing the results I have acquired to results previously made by Pim [17], the threshold distribution over all matrices has better statistical results when a larger dataset is taken and a box is placed over the pixel chip that eliminates any outside disturbance as expected. Implementing the amount of DAC steps to be 60 and setting the other user settings to the standard values lead to promising figures which showed that there were hardly any pixels that were 'dead' or that did not function. Overall, the thresholds are pretty well defined among all the pixel matrices, which shows that the pALPIDE v2 chip works properly in our experimental setup.

3.4 Noise Measurements

Along with threshold scans, the noise of a pixel can also be determined. The difference between the threshold and the noise is that the threshold is the charge that has to reached in order to register a hit and the noise is how much the threshold can be lowered until a hit is registered. Noise can be calculated by taking the derivative of the error function that is fitted to the threshold scans. This results in a Gaussian curve of which we can calculate the width, which is then the noise for that pixel. In the following figure, the noise distributions are plotted for all the different pixel matrices.

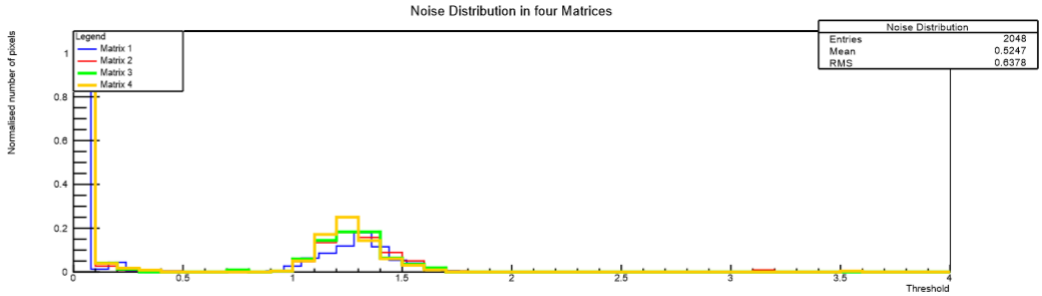

Figure 3.3 – The noise distribution in the four matrices

As can be seen in the figure above, there is a strong peak at 0. This peak is there due to statistical errors in calculating the noise for different pixels. Some derivatives and Gaussian fits do no work properly and therefore give unexpected results. Yet, apart from the fitted functions that do not work properly, the noise is also well defined along all of the different pixel matrices. It can be seen that the noise is constant across al different pixel matrices. This is promising since this would mean that the noise is very well

defined and can thus be taken into account when doing measurements with this pixel chip.

Concluding, these statistical analyses in ROOT show that the pixel chip performs well in our experimental setup. Using a box to prevent outside factors from influencing our measurements, setting the right standard settings and gathering a large dataset, it has been found that the threshold and noise measurements for this pixel chip provide a solid basis on which it can be said that this prototype of the ALPIDE chip works properly. This gives some assurance that future models of this pixel chip will work even better and that when these pixel chips will be installed as part of modules in the ITS, they will generate data that is accurate enough for to follow the physics goals set by the ALICE group for the coming years.

Chapter 4

Connection testing

4.1 Outer Barrel module testing

The previous chapter has covered the analysis of one single pixel chip. However, this is of course not realistic since whole modules of 7 by 2 pixel chips will be be installed in the ITS. Nikhef has taken responsibility to provide a module testing system that can be used at all stave production sites. This means that the machine that will be chosen has to be user friendly as well as produce accurate results. Specifically, different research groups have to be able to use the module tester right away without doing major modifications to it. Also, the testing of different modules should not take much time since a lot of modules have to be tested individually.

Two different types of machines have been researched in order to find the right one to provide larger scale testing of modules. The first on is the industrially made Romex Probing machine that tests modules as a whole. Secondly, we have the Flexible Printed Circuit board Cutter (FPC) which is specifically developed to provide the cutting of a silicon module in order to connect an external connector which can be used to gather data from a whole module. During the course of my bachelor research a choice needed to be made between the two different machines. In the end, the FPC was chosen due to a number of reasons. All figures provided of the Probing machine and the FPC cutting machine are from the Nikhef website of the ALICE group. [20]

4.2 Probing machine

The company Romex supplies industrially made test fixtures for testing Printing Circuit Boards that guarantee high quality testing of precise electrical systems. This precise testing can only be done when there is a reliable connection between the testing system and the unit under test (UUT). Since the modules we are testing supply data which has to be read out very precisely, minimal loss or distortion of the electrical signal has to be present in order to properly test the modules. The Probing machines Romex supplies provide room for customisation and have therefore been chosen to test modules with.

4.2.1 Specifications

The model used for testing modules at Nikhef is the MG02 model from a series of test fixtures that the Romex company supplies. Its dimensions are 470 x 490 x 170 mm (WxDxH) thus it can fit on a table top [21]. The precision and reliability of the connections that are made between the machine and the module depends on the mechanical construction of the machine. Hence, the Probing machine is made out of solid aluminium parts. Especially the parts that push down the module onto the connection pins has to be precise, and that is why these are made of solid aluminium as well.[21]

The main feature for connectivity between a module and an external device is a linear click system with a ball bearing and sliding sleeve. The modules that are put

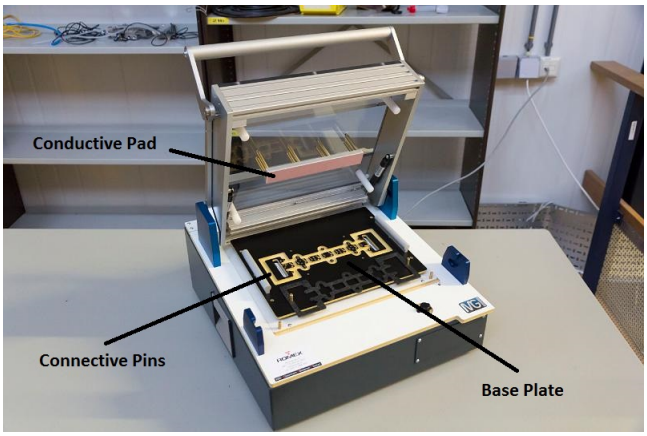

Figure 4.1 – The customised Romex probing machine featuring conductive pressing pad and a base with holes and sleeves for positioning

in place on the Probing machine are connected by these spring powered contact pins. These pins have an accurate linear movement of 15mm, which provides enough space for the modules to be contacted from the top and the bottom at the same time. The spring system in the connective pins makes sure that all connections between the module and an external measuring apparatus is made for all connection places on the module [21]

4.2.2 Testing Procedure

In order to test a single module, it has to be put in place in the probing machine and pressed down onto the connective pins. Before this can be done some modifications have to be made in order to prepare to Probing machine to properly test the modules that are available to us at the moment. As can be seen in the provided picture, the position of the module is held in place by a base which features holes and sleeves. This provides a fixation of the module with an accuracy of about 3mm. On the top we can find a thermal conductive pressing pad which can absorb a thickness difference of about 0.4 mm. This is used to press the module firmly into place on the base plate. It needs to be thermally conductive since when a module is tested it generates heat during the half hour it is being tested. In fact the module produces 70 mW/cm^2 * (21.1*3.1) cm^2 = 4.5 W of heat, so it needs extra external air flow or water cooling as well along with the thermally conductive pad in order to test the module under the correct conditions.

4.2.3 Advantages and disadvantages

The advantages of this system are that it is easy to operate. Since the the only steps needed to electronically test a module are to place it on the base plate and then press down with the conductive pad in order to connect all connection ends of the module to the pins in the Romex machine. However, this pressing down on the module provided several issues. Firstly, since the material of which the conductive pressing pad is made is probably some carbon based material. When pressing down on the silicon top of the module, this leaves traces of carbon on the sensitive silicon surface. After inspecting with a microscope it has been concluded that traces of the carbon from the conductive pad are left on the silicon layer, obstructing the possible detection of particles. This is of course not desirable, since the silicon layer has to perform with optimal precision and without obstruction of outside dust or these carbon traces.

Another disadvantage of the Romex probing machine is that the base plate was not completely flat over the whole surface of the module as we can see in the picture below. This caused the damage of one of the tested modules since the pressure of the conductive

pressing pad could not be withstood by the module.

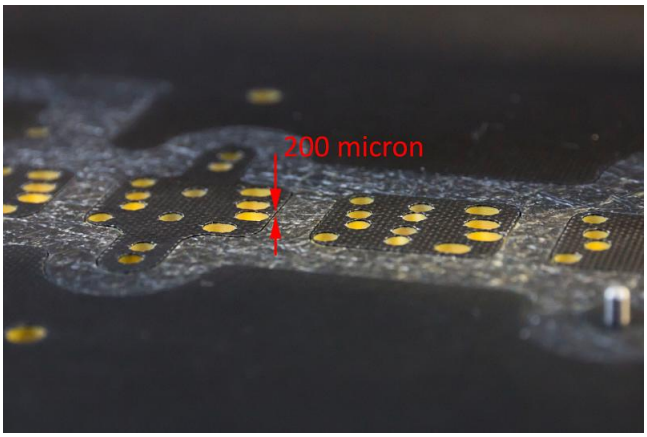

Figure 4.2 – Base with holes and sleeves for positioning with height difference of 200 microns

The connections of the module with the machine also did not work properly. As can be seen in the figures below, the module has connectivity issues due to the pins not being aligned properly with respect to each other. This causes some of the connecting ends of the module not to be connected properly to external cabling.

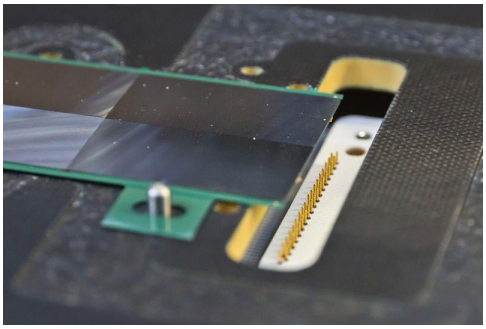

(a)

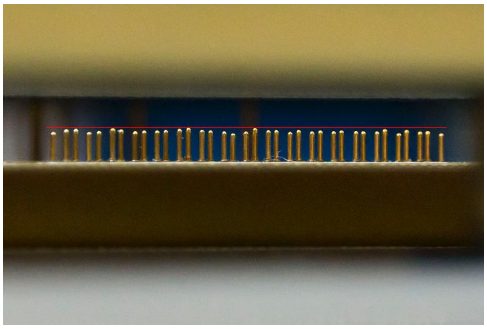

(b)

Figure 4.3 – Left a module placed on the base plate for testing, on the right the connector pins that are not aligned properly

In conclusion, the Probing machine had too much challenges that still had to be overcome before it can be used on large scales and that is what made us decide not to use this machine as the one that is going to be used for module testing. Therefore, all focus went to developing the FPC cutting machine, which was being researched simultaneously. The next section will cover the FPC, its characteristics and why this type of module tester is being developed further at the moment instead of the Probing machine.

4.3 FPC Cutting machine

Since the Probing machine did not meet the standards of becoming the machine that will be used by other research groups in order to test their modules on a larger scale, the other option has to be developed further. The FPC cutting machine uses a whole different approach to module testing than the probing machine. The principle on which the FPC cutter works is that a cut is made right next to the silicon covered part of the module in order to connect and external connecting piece to it as in the next figure.

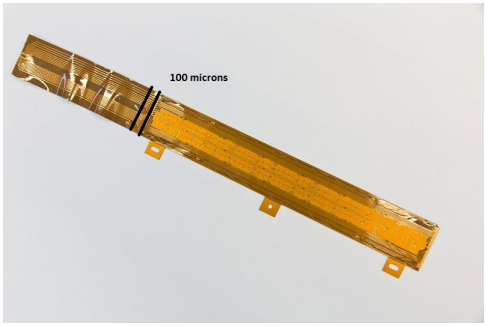

Figure 4.4 – A module with an external connector attached to it.

This cutting procedure has to be done with very high precision in order not to damage any silicon pixel chips. 100 microns is the limit between which the cut has to be in order not to damage the silicon side and make it possible for a module extension to be connected. The next section will cover the different aspects of the cutting machine and how they all contribute to cutting with a straightness within the set limits that have to be met in order not to damage the entire module beyond repair. In the figure below, we can see a schematic as well as a real picture of the design of the FPC cutting machine.

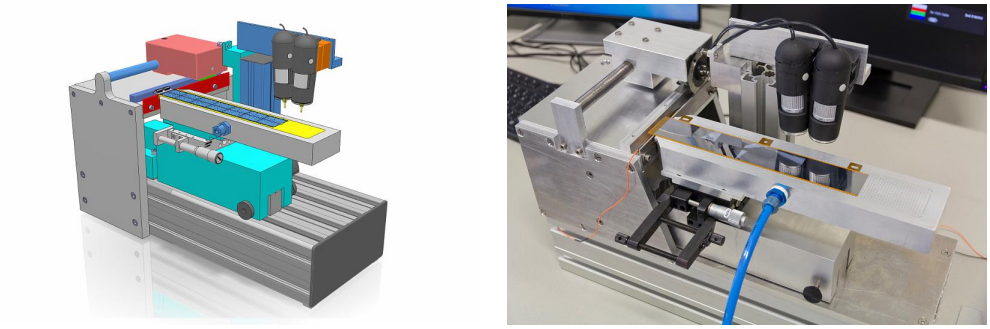

(a) **(b)**

Figure 4.5 – Left schematic of the FPC, on the right a picture of the actual FPC at Nikhef

4.3.1 Cutting Precision

As mentioned before, the primary goal of this machine is to perform cuts as straight as possible. Or at least within the set limits that will not damage the silicon layer of the pixel chip. The cut has to be made within a range of 100 microns. The actual gap between two modules in a stave is actually 200 microns. However there are two different factors that have to be taken into account in this situation. Firstly there is the uncertainty of the straightness of the edge of the module during production. This uncertainty is also within the range of 100 microns. Added to that, the cut is also not completely straight. Hence both parties have to share this gap of 200 microns evenly.

Just to be safe, a mean precision of 50 microns is desired to be achieved when using this cutting device even though the cut only has to be made within a 100 micron gap. Two different types of measurements are done in order to see whether or not the cut is straight enough. This is the straightness, defined as the maximum distance between the two points which are furthest apart on the line of the cut. Since the cut is not completely straight, this is a clear indication to see if the cut is within the limit of 50 microns. However, since the cut can be straight enough but it can be at a large angle with respect to the edge of the silicon, the perpendicularity has be be measured as well. Perpendicularity is defined as the maximum deviation the cut has with respect to the edge of the silicon. Perpendicularity can be measured with a line that has an angle of 90 degrees with respect to the long side of the silicon edge of the chip. The illustration

below shows these principles with the red line indicating the straightness and the blue line indicating the perpendicularity. Note that this example is exaggerated in order to illustrate the difference.

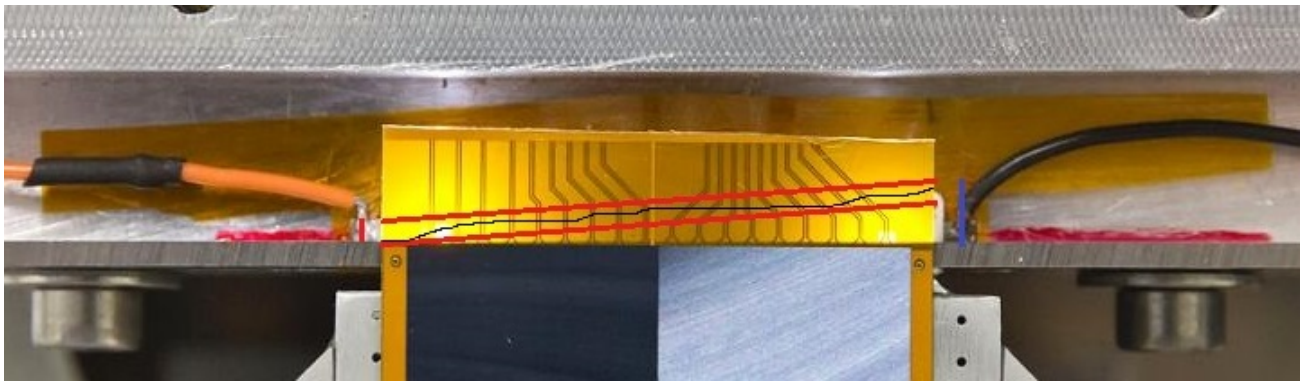

Figure 4.6 – Straightness of the cut measured in two ways. Red indicating straightness and blue indicating perpendicularity

Straightness and perpendicularity are both measured using the Mitutoyo Coordinate Measuring Machine which is a high precision industrial measuring machine. The results are then analysed to see if the cutting machine cuts straight enough. Now that the standards have been set for the straightness of the cut, the features of the cutting machine that provide this accuracy are discussed.

4.3.2 Positioning structure

First of all the cutting device needs to be built on a strong and stiff basis. The stiffness of the construction is particularly important to the straightness of the cut since the forces that are applied when cutting should not move the module out of its intended place.

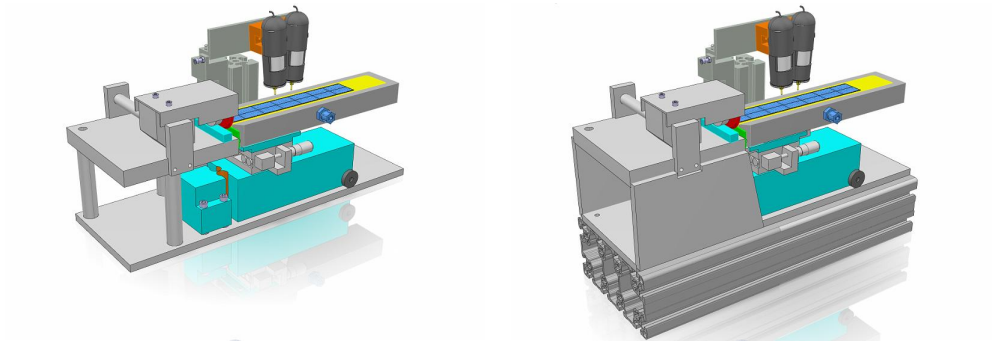

(a) **(b)**

Figure 4.7 – Left shows the cylindrical aluminium beams that support the sturcture of the FPC. Right is added aluminium plates on the outside for stiffness.

This positioning table also provides translational and rotational movement in order to position the module as precise as possible before the cut is made. The following illustration shows the translation and rotation tables onto which the vacuum table is mounted. These translational and rotational movements can be adjusted very carefully using screws that can be tightened in order to move the vacuum table.

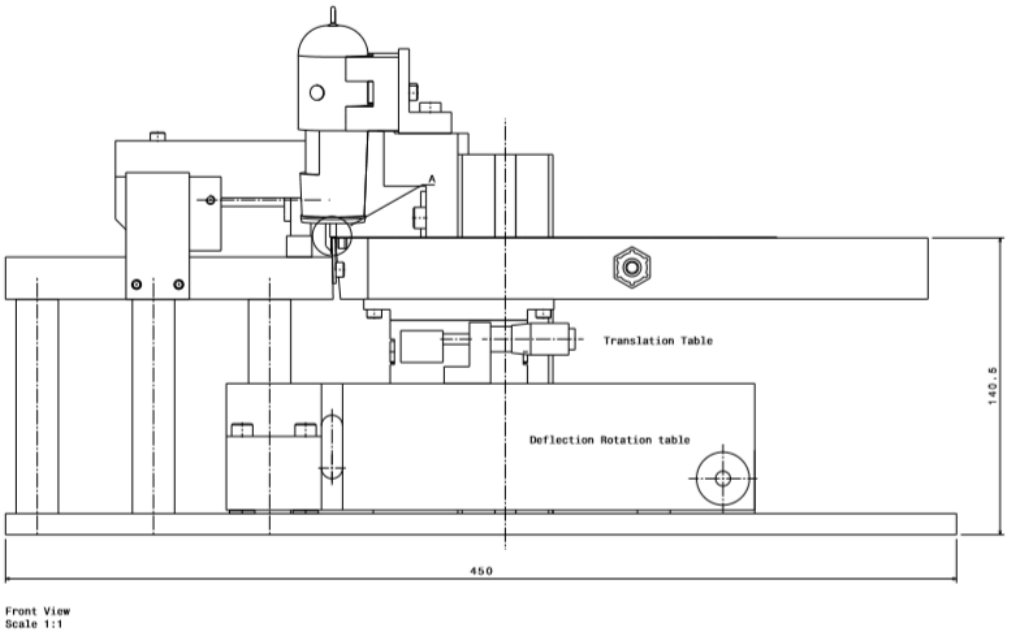

Figure 4.8 – Translation and rotation table for the FPC cutting machine

Which brings us to the vacuum table itself. It features a horizontal plane onto which the module can be placed. This plane has small holes in it that are connected to a vacuum pump. Over the total area of the module, the vacuum pump forces it to stay in place during cutting. Currently, the vacuum table is larger than the module, which creates a vacuum leak at the edges of the vacuum table. This is solved by placing a thin foil over the module which covers the whole area of the vacuum table in order to properly provide suction power to keep the module in place.

4.3.3 Alignment Microscopes

As can be seen in the above pictures, two microscopes can be hovered above the cutting region in order to do the final adjustments to the module before cutting. Points on the module have been chosen that indicate whether or not the module is in the correct position to start cutting. These two microscopes are connected to a computer using a USB cable. It would be favourable to have both microscopes simultaneously transmitting images to the computer screen. The software provided with the microscopes does not support both cameras at once. Hence new software has to be written in order to provide this function. Another function that the cameras have is that they are hovered over the cut once it is done. This is mainly to see if there are any large abnormalities in the region that has been cut. A more detailed inspection of the cut is done with specialised measuring machines such as the Mitutoyo measuring machine.

Another function that is built in the FPC cutting machine is LED lights under the cutting area. Because the module sticks out over a gap between the vacuum table and the cutting wheel, the LED's cast a shadow of the knife. These added LED's can be seen in the following picture. This makes it possible that there are two reference points which can be used to properly align the module with the two microscopes before cutting. These are the silicon edge and the shadow of the knife.

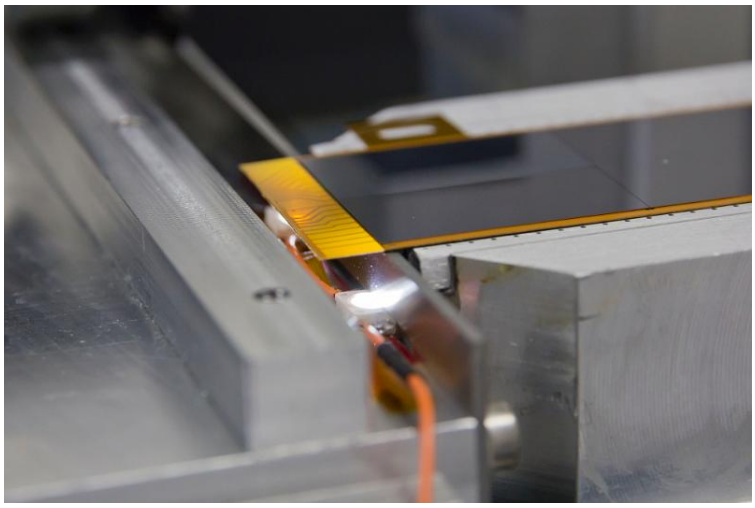

Figure 4.9 – LED's that have been installed under the cutting area in order to provide a shadow which can be used for referencing

4.3.4 Cutting wheel

With the main function of the FPC cutting tool being of course cutting, the knife and cutting wheel are essential to the design of the apparatus. The way this mechanism works can be explained with the following picture of the cutting machine in action.

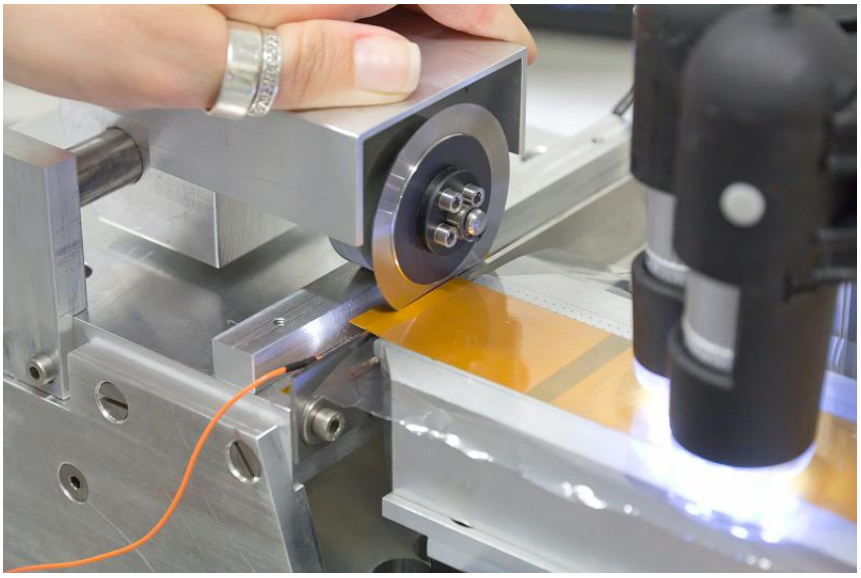

Figure 4.10 – Cutting wheel cutting a module

We can see in the above picture that the cutting wheel is guided by a support structure which is mounted on a axle that this structure can freely move on. Inside this structure is a spring around a cylinder that is directly connected to the cutting wheel to make sure the cutting wheels is always firmly pressed against the knife. This provides a straighter cut along the length of the module. Also, there is a very slight angle of 1 degree between the knife and the cutting wheel to provide optimal cutting.

4.3.5 Flipping the module

Another challenge in module testing is that the modules have to be flipped in order to be placed silicon side up on the vacuum table. The reason that the silicon side has to face upwards is that any contact between the delicate silicon layer of the module and

the vacuum table could damage the pixel chips permanently. In order not to damage the module when it needs to be flipped, a vacuum suction tool has been developed that can safely turn over the module when it needs to be flipped. The flipping tool consists of vacuum pump powered rubber gripping pads that divide the suction power over the whole module.

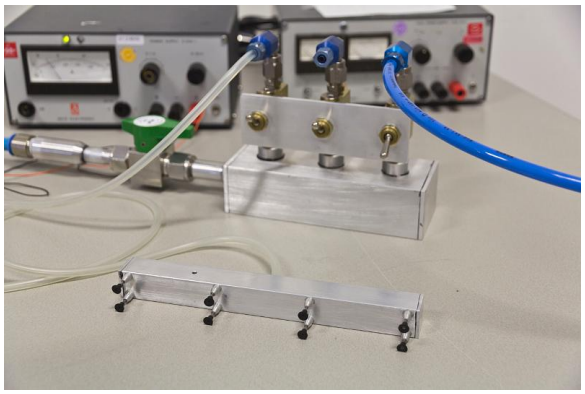

Figure 4.11 – Custom tool that has been disigned to flip individual modules when necessary

4.3.6 Results

During the development of the FPC cutting machine, several test cuts have been made in order to determine what parts of the machine still needed improvement. Data is gathered by using a high precision Mitutoyo Coordinate Measuring Machine, which measures x and y locations of points on the edges of the cut. Using the raw ASCII data from the Mitutoyo, I have made plots in ROOT to examine if the straightness of the cut meets the standards of being within a limit of 100 microns.

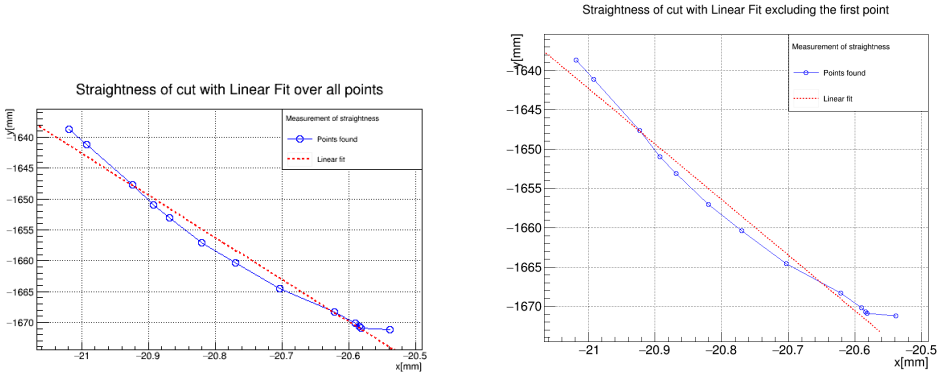

(a) **(b)**

Figure 4.12 – Two plots of the straightness. Left over all data points, right excluding the first data point.

The left plot is a graph taken over all the points that were in the data file including a linear fit over all points. The right plot shows a linear fit through all points except the first data point which shows to deviate a lot from all the other data points. This is probably due to the module moving slightly when the cutting wheel first hits the module. Another explanation could be that the Mitutoyo machine measured this data point incorrectly, however I presume this explanation to be less likely.

Even with the first data point excluded from the dataset, the maximum deviation from the linear fit over all the data points show to be more than 100 microns. Hence, this cut would not meet the standards set for the straightness of a cut. After doing

this statistical analysis in ROOT, it has been found that the dimensions over which the data points have been gathered do not correspond with the dimensions of the edge of the module. This means that the Mitutoyo measurement was not over the whole edge of the module. Although this could be of influence on the straightness of the cut, the first data points clearly show that the cut is not within the 100 micron limit that has to be achieved. So, improvements had to be made to the FPC. These improvement are listed in the previous paragraphs.

The research and development phase continued after these initial results. All of the above features like the alignment microscopes, the positioning table and LED's were added to the design of the FPC cutting machine. Added to that, the machine was placed in a clean room at Nikhef to prevent any dust from influencing the measurements. This resulted in significantly better cuts. The results are listed in the table below. In total, three cuts were done after all these upgrades were done in order to be certain that the FPC cutting machine works properly. Note that the first measurement is done with a different measuring machine, namely the Zeiss measuring machine. This is done in order to be sure that the values found for the straightness and perpendicularity are consistent across multiple measuring machines.

Measurement Device	Distance from silicon (mm)	Straightness (mm)	Perpendicularity (mm)
Zeiss	0.04	0.015	0.04
Mitutoyo	0.054	0.021	0.019
Mitutoyo	0.035	0.021	0.020

From these results it can be concluded that after all the modifications, the FPC cutting machine cuts within the 100 micron range that it need to be in between. This is a very promising result since this means that the current version of the cutting machine would be capable of preparing FPC's for connection to an extension with which data analysation can be done for the whole module. The future plans for this cutting machine is that it can be used with ease by different research groups that will do stave production. To make possible, several modifications have to be made in order to make it even more user friendly. For instance, a cover that makes it impossible to cut one's fingers on the knife is proposed to be made. Along with that, a software upgrade is going to be made that supports both cameras at once on one computer. Also, a more user friendly Graphical User Interface is going to be developed to make certain tests like the register and threshold test easier to do for whole module testing. In conclusion, we can safely say that this current model is capable of doing cuts that have a straightness and perpendicularity that is within the 100 micron range. A mean value of 50 is aspired since that will ensure that the cut is within the given limit, and this requirement is also met as can be seen from the measurements on the last cut. In the coming months, the FPC cutting machine that was developed at Nikhef will be distributed to 5 different research centres that will perform the module testing and assembly.

Chapter 5

Conclusion

In conclusion, the current attempt in unifying all forces and particles into one system called the Standard Model of Physics is far from complete. While the model describes the interaction between fermions that interact via the Strong, Weak or Electromagnetic interaction and their accompanying bosons. Gravitation, Dark Mass and Energy and the origin of mass are phenomena that are not covered by this model. Furthermore, we have seen what the current specifications of the ALICE ITS are and what can be improved upon the experimental setup at CERN. The main research areas of the ALICE detector are all particles that are created after the formation of a Quark Gluon Plasma. Analysing secondary effects that arise from the QGP such a jet quenching and strange particle production can reveal the properties of this relatively unknown phase of matter called the QGP. Since a second Long Shutdown of the LHC is planned to take place in 2018 and 2019, the opportunity arises to update and improve upon the current detector experiments at CERN.

A major part in the upgrade of the ALICE detector is installing a new Inner Tracking System (ITS). The ITS is the detector element that is closest to the beam pipe so it has the best chance of detecting particles with short decay times which can be used to study a QGP. The upgraded ITS features seven layers of Silicon Pixel Detector (SPD) which will have a higher pixel resolution and improved data read-out system in the form of the ALPIDE architecture. Some other improvements are that the first detection layer is placed closer to the beam pipe and the layers will have a lower material budget. All these upgrades make it possible for the ITS to better analyse low momentum particles that have been formed after a QGP has been created.

At Nikhef, a prototype version of the ALPIDE chip is being tested for threshold and noise to see whether or not all the different pixels work properly before they are installed at the ITS. Statistical analysation of a large dataset that has been gathered using previously written software and the most optimal circumstances, reveals that the pALPIDE v2 chip performs well in threshold and noise tests. This is a promising prospect for later prototypes of the ALPIDE chip. Since it will not be individual chips that will be installed, but 7 by 2 chips assembled into a module, these modules also have to be prepared for testing. Two machines, the Probing machine and FPC cutting machine underwent initial tests to see which of the two was more suitable for mass scale module testing. Listing advantages and disadvantages, a choise has been made to further develop the FPC cutting machine and abandon research and development of the probing machine. Initial test of the cutting machine showed cuts that were not within the limits of accuracy that it has to be. So, multiple upgrades to the FPC have been installed in order to make the cut more precise. After a positioning structure, alignment microscopes and guiding LED's were added, the cut was significantly better than the first test. The initially set requirements for the straightness and perpendicularity of the cut have been achieved, making the FPC a suitable candidate for mass scale module testing and assembly. However, development is still going on in order to improve the user friendliness of the FPC.

Chapter 6

Acknowledgements

Many thanks go out to Paul Kuijer, Panos Christakoglou and Dimitra Andreou at Nikhef for being ready to answer all my questions concerning C++ programming, ROOT and giving me feedback on my presentations an writing. The weekly group meetings were always fun to be in and very informative for me. A large portion of this thesis comes from the discussions we had in the group meeting but also with Gerrit and Marco who were responsible for the mechanical engineering of the Probing machine and the FPC cutting machine.

In addition to this, I would like to add that I have learned a lot about world politics since the usual discussions about the governments of Greece, Turkey and Iran were always held during the lunch at Nikhef. These four months I have spent at the ALICE group at Nikhef have gone by very fast and I have learned a lot thanks to everyone involved with my Bachelor Research.

Bibliography

[1] Wikipedia page on Standard Model, https://en.wikipedia.org/wiki/Standard_Model, 2016

[2] Wikipedia page on Strong Interaction, https://en.wikipedia.org/wiki/Strong_interaction, 2016

[3] Wikipedia page on Higgs Symmetry, https://en.wikipedia.org/wiki/Higgs_mechanism, 2016

[4] Dark Energy, Dark Matter, http://science.nasa.gov/astrophysics/focus-areas/what-is-dark-energy/, 2016

[5] Frank Wilczek, *QCD Made Simple*, Physics Today, 2000

[6] Wikipedia page on Quantum Chromodynamics, https://en.wikipedia.org/wiki/Quantum_chromodynamics, 2016

[7] Rajan Gupta, *Introduction to Lattice QCD*, Los Alamos National Laboratory, 1998

[8] Manuel Caldern de la Barca Snchez, *Phase diagram QGP*, https://www.bnl.gov/rhic/news/050807/story1.asp, 2007

[9] Heavy ions and quark-gluon plasma by CERN group, http://home.cern/about/physics/heavy-ions-and-quark-gluon-plasma, 2016

[10] Yukinao Akamatsu and Shuichiro Inutsuka, *A new scheme of causal viscous hydrodynamics for relativistic heavy-ion collisions: A Riemann solver for quark-gluon plasma*, 2013

[11] Cian O'Luanaigh (CERN), *Proton beams are back in the LHC*, 2015

[12] Florent Fayette, *Strategies for precision measurements of the charge asymmetry of the W boson mass at the LHC within the ATLAS experiment*, http://inspirehep.net/record/823897/plots, 2009

[13] Wikipedia page on ALICE, https://en.wikipedia.org/wiki/ALICE:_A_Large_Ion_Collider_Experiment, 2016

[14] Vito Manzari for the ALICE group, *The present Inner Tracking System - Steps forward!* http://alicematters.web.cern.ch/?q=ALICE_currentITS, 2012

[15] The ALICE Collaboration, *Technical Design Report for the Upgrade of the ALICE Inner Tracking System*, 2014

[16] Corrado Gargiulo for the ALICE group, *ITS Upgrade Project: Mechanical and Cooling Structure (Working Group 4)*, http://alicematters.web.cern.ch/?q=ITSUpgrade_WG4, 2012

[17] Pim Verschuuren, *Testing the pALPIDE v2 chip for the upgrade of the ALICE Inner Tracking System*, 2016

[18] Lukas Arts, *Alpide Testing Software*, 2016

[19] P.Yang, G. Aglieri et al, *MAPS development for the ALICE ITS upgrade*, 2014

[20] ALICE Group at Nikhef, http://www.nikhef.nl/pub/departments/mt/projects/AliceUpgrade/, 2016

[21] ROMEX website, https://www.testprobes.nl/romex/, Romex company, 2016